Direct Observation of a Smectic Bilayer Microstructure in Side-Chain Liquid Crystalline Diblock Copolymers

Mitchell Anthamatten, Jung-Sheng Wu, and Paula T. Hammond*

Department of Chemical Engineering, Massachusetts Institute of Technology, 77 Massachusetts Avenue, Room 66-550, Cambridge, Massachusetts 02139-4307

Received July 6, 2001; Revised Manuscript Received September 5, 2001

ABSTRACT: TEM analyses enable a priori investigation of smectic bilayer structures in an amorphous−liquid crystalline (LC) diblock copolymer. A newly synthesized copolymer with 85 wt % LC phase segregates into a layered morphology in both bulk and thin film studies. The microstructure has a periodicity of ∼70 Å and forms highly ordered micron-size monodomains. SAXS, TEM, and AFM data suggest that the LC domains consist of smectic bilayers, and amorphous polystyrene domains are present as disklike domains that arrange hexagonally between smectic bilayers. Temperature-dependent SAXS experiments and quenched TEM micrographs indicate that a reversible change in microstructure occurs at the LC clearing point. These observations confirm that, at high LC volume fractions, side-group ordering has a greater affect on block copolymer microstructures. Our results are contrasted to recent theoretical predictions of block copolymer microstructures.

Introduction

Side-chain liquid crystalline block copolymers offer great potential to serve in a wide array of commercial applications. Furthermore, they combine the thermotropic ordering of liquid crystals with the physics of block copolymer phase segregation. Understanding the overlap of these two self-assembly phenomena has been a common goal among several research groups.[1−9] We have previously reported the synthesis and LC phase behavior of well-defined diblock copolymers of styrene and a methyl methacrylate monomer with a biphenyl benzoate mesogenic side chain (PS-HBPB).[2,3,10] Through X-ray analysis and optical microscopy, we have observed chiral smectic C* structures at temperatures as high as 170 °C.[2,3] Also, using SAXS and TEM, we have investigated the diblock's morphology by varying the LC volume fraction and the total molecular weight; a summary of these morphologies and the chemical structure of the polymer is shown in Figure 1.[2] Key features include the absence of LC cylinders, an unusually broad lamellar regime, and the presence of transitional morphologies at nearly equal volume fractions. We have also observed that LC phase transitions can induce block copolymer order−disorder and order−order transitions.[1]

In the analysis to follow, we discuss the morphology of a newly synthesized sample, PS-HBPB85, also plotted in Figure 1. Considering PS-HBPB85's high LC content, on the basis of classical block copolymer phase diagrams,[11] one would expect amorphous cylinders or spheres; however, we present experimental evidence supporting the following microstructure: hexagonally packed amorphous polystyrene (PS) disklike domains that are separated by an LC smectic bilayer (S_{C2}) substructure that is oriented homeotropically to the block copolymer interface.

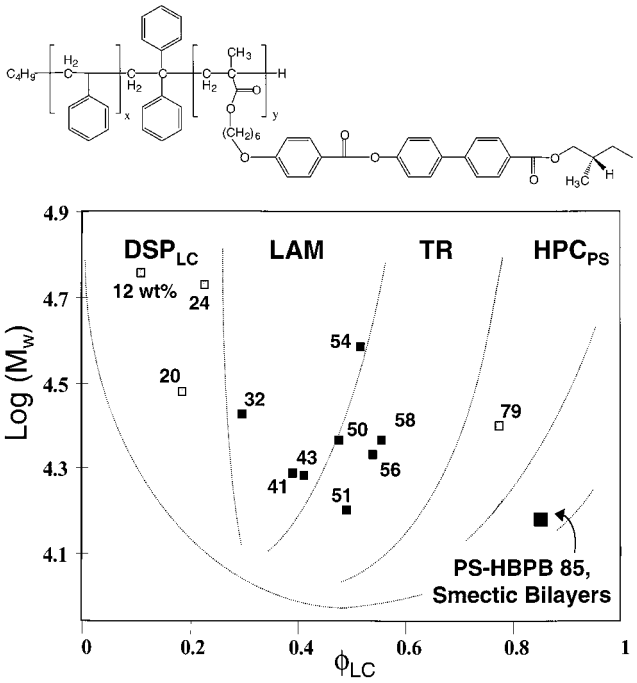

Figure 1. Composition vs molecular weight phase diagram indicating observed block copolymer morphologies for PS-HBPB samples. The following morphologies are observed: dispersed LC spheres (DSP), pure lamellae (LAM), transitional morphologies (TR), hexagonal-packed cylinders of PS (HPC$_{PS}$), and a morphology consisting of smectic bilayers. The inset shows the molecular structure of the PS-HBPB diblock copolymers.

Experimental Section

The synthesis of PS-HBPB85 involved sequential anionic polymerization of styrene followed by a mesogenic monomer and is reported elsewhere.[10] To ensure complete removal of PS homopolymer, the sample was further purified by a preparative GPC method using THF as the mobile phase. The resulting molecular weight distributions were characterized using a Waters' PS-calibrated GPC system. The number-averaged molecular weight for the PS block is 1.7 kg/mol and for both blocks is 12.1 kg/mol; PS-HBPB85's polydispersity is 1.09. Wide-angle X-ray analysis, polarized optical microscopy, and temperature-dependent SAXS experiments confirmed the existence of a chiral smectic C* structure in this series of diblocks[1,2,10] at temperatures as high as 170 °C.

TEM. Films were slowly cast from 3 wt % solution in tetrahydrofuran and dried under vacuum for 2 days. To

10.1021/ma011168n CCC: $20.00
Published on Web 10/20/2001

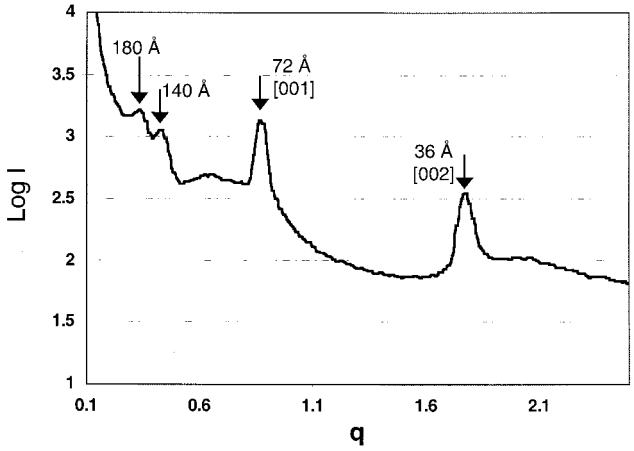

Figure 2. SAXS 1D line integrals of PS-HBPB85. Data are plotted as the logarithm of the relative scattered intensity log $I(\mathbf{q})$ vs the scattering factor $\mathbf{q} = (4\pi \sin \theta)/\lambda$, where $\mathbf{q}$ is one-half the scattering angle and λ is the X-ray wavelength.

encourage phase segregation, the films were annealed at 110 °C under vacuum conditions for 2 and 7 days. Following annealing, fragments of the films were embedded in epoxy and sectioned using an RMC ultramicrotome (model MT-X) equipped with a diamond knife. Specimens were then collected on copper TEM grids and stained for 1 h with RuO_4 vapor. Transmission electron microscopy was performed under bright field with an accelerating voltage of 200 kV.

SAXS. Small-angle X-ray scattering was conducted using a computer-controlled Siemens X-ray system. The collimated X-ray beam, consisting of Cu Kα radiation ($\lambda = 1.54$ Å), was passed horizontally through an evacuated chamber onto a 2D xenon detector. Samples were placed in a sealed thin-walled capillary tube that was suspended 63.4 cm away from the detector in a hotstage (Instec, model HS250) that was modified for operation under vacuum conditions. Data were acquired as scattered X-ray intensity, I, taken as a function of temperature and the scattering vector, $\mathbf{q} = (4\pi \sin \theta)/\lambda$ where θ is one-half of the scattering angle.

AFM. AFM analysis was then performed using a Digital Instrumental Nanoscope IIIa in D3000 standard tapping mode.

Results and Discussion

Bulk Morphology. Solvent cast films of the LC−amorphous diblock copolymer PS-HBPB85, shown in Figure 1, were examined using TEM and SAXS. A 1-D SAXS diffraction pattern at room temperature is shown in Figure 2. Two intense Bragg peaks occur at integral multiples of the scattering vector, indicating a highly periodic structure. This periodicity was measured to be 72 Å, nearly twice that of the smectic layers observed in other diblocks of the same series with lower LC content, the LC homopolymer, and analogous low molar mass LC mesogens.[3] Two weaker Bragg reflections are present at 180 and140 Å and indicate a larger secondary structure.

A typical TEM micrograph of PS-HBPB85 following a 2 day annealing period is shown in Figure 3a. The thin, dark bands are RuO_4-stained PS domains, and the white bands are LC domains. Careful examination of such images at higher magnification shows that the PS layers are highly perforated, and the LC phase is continuous. From these images, the layer periodicity was determined to be 65−70 Å, which agrees well with X-ray results.

Figure 3b contains a second TEM micrograph of the same sample annealed for 7 days instead of 2. Extended annealing enhances the layer order, and grain sizes are

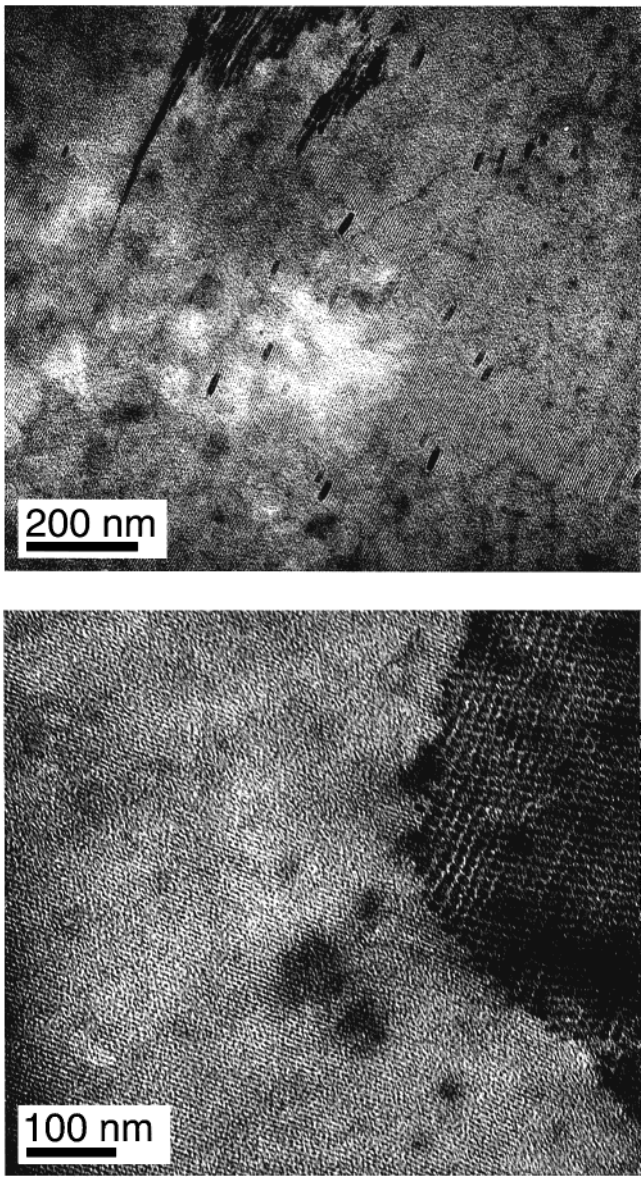

Figure 3. TEM micrographs of PS-HBPB85 following annealing at 110 °C for (a) 2 days and (b) 7 days.

observed on the order of tens of microns. *Two* ordered structures, both appearing in 3b, were identified through TEM: (1) the PS-perforated, smectic bilayer structure discussed above and (2) a hexagonally packed structure. The lattice spacing of the hexagonal order was measured to be 130−170 Å and corresponds well to the lower angle SAXS diffraction peaks shown in Figure 2. However, these peaks appear diffuse and alone do not yield sufficient information to confirm a hexagonally packed structure. During TEM analysis, samples were also tilted ±30°, but the 3D shape of the larger-sized polystyrene domains could not be inferred. Hexagonal patterns similar to those in Figure 3b also appeared following the short (2 day) annealing times, but their grain sizes were much smaller and the hexagonal lattice was not as clear. Our experiments indicate that PS-HBPB85 takes days to fully develop its morphology. Lamellar growth and defect annihilation are kinetically slower than in amorphous−amorphous diblocks. Here, the LC backbone mobility is reduced by the highly viscous smectic ordering of side groups.

Comparing PS-HBPB85's bulk periodicity of 70 Å to the estimated all-trans side-chain length of 35 Å sug-

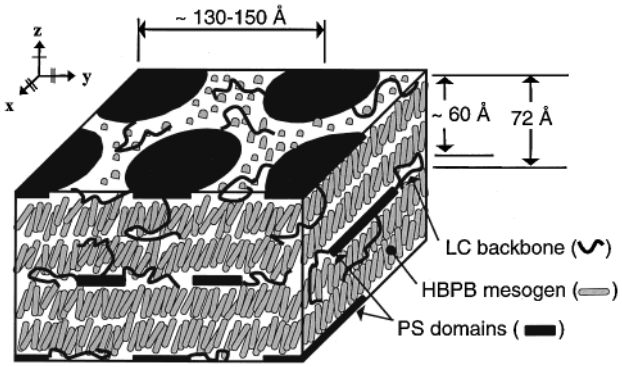

Figure 4. Cartoon showing proposed LC block copolymer superstructure: side-chain LC's form bilayers that are separated by flattened spheres or disk-shaped polystyrene domains.

gests a tilted, smectic C bilayer phase (S_{C2}) as indicated schematically in Figure 4. In this cartoon, the polystyrene microdomains appear as disks, or highly oblate spheres, that have been deformed due to smectic ordering in the LC block. These disk-shaped PS domains arrange hexagonally into planes and are sandwiched between adjacent smectic bilayers. When viewed from the *x*- or *y*-directions, the perforated lamellar layer structure is visible, and when viewed from the *z*-direction, the hexagonal arrangement is observed. Both of these perspectives are evident in the grains shown in Figure 3b. The S_{C2} mesophase described here is similar to that observed in a variety of LC side-chain homopolymers including polyacrylamides,[12−14] poly(vinyl ether)s,[15] poly(glycidyl ether)s,[16] and poly(methylsiloxane)s.[17] In these systems the LC backbone partitions the mesogens into bilayers, whereas in the current study, the PS disklike domains separate adjacent bilayers.

Using PS-HBPB85's composition, bulk density, and the measured lattice spacings and considering the monodisperse 1.7 kg/mol (∼16 repeats) PS block, we expect one disk to consist of about 75 PS chains. Also, considering the limiting case where the disk diameters are 70 Å and a layer periodicity of 72 Å, an analysis of the unit cell geometry shows the thickness of the PS domains is 14 Å, which is smaller than the PS block's calculated unperturbed radius of gyration of 28 Å. Thus, the PS chain is believed to assume an entropically penalized pancake conformation. Likewise, the LC domains are estimated to be at most 61 Å thick, and considering the lengths of an all-trans side-chain, in such a geometry a smectic bilayer structure would require mesogens to be tilted a minimum of 29° from their layer normal. This tilt angle estimate agrees well with our earlier measurement of 30° in higher molecular weight block copolymers of the same type.[2]

It is interesting to note that, in the proposed S_{C2} structure, the smectic layers run parallel to the flat surfaces of the PS disks, i.e., in the *x*- and *y*-direction. For samples with lower LC volume fractions, and higher molecular weights, the smectic layers are usually perpendicular to the block copolymer interface due to the extension of the LC backbone away from the block copolymer intermaterial dividing surface.[2] The parallel arrangement observed here has only been seen in bulk (thick films) for polymers with a decyl spacer, where the mesogen was decoupled from the backbone.[18] Parallel arrangements have also been reported in ultrathin film studies of these[19] and other LC block copolymers.[20] In ultrathin films, the high-energy air−polymer interface encourages mesogens to anchor homeotropic to the interface. In this study, the S_{C2} structure is arranged parallel to the PS disks in order to form large continuous LC domains, thereby optimizing the number of mesogen−mesogen lateral interactions. Also, per Figure 4, most of the copolymer junction points are likely located on the edges of the PS disks. This enables full segregation of the two blocks and does not require LC backbones to cross smectic layers. Furthermore, it allows the nonpolar LC end groups to contact one another in the middle of the LC bilayers, and the LC backbone may occupy the less dense regions of space between adjacent PS disks. Last, if all the copolymer junctions were located on the edges of PS disks, the side-group density would be lowest directly above and below the flat surfaces of the disks. To avoid density fluctuations, one would expect adjacent planes of hexagonally packed disks to be staggered. Indeed, through our TEM analysis, staggered disks were identified when viewed from the *z* direction.

Clearly, the TEM images indicate that PS-HBPB85 forms well-ordered, micron-size domains with little curvature. These observations are contrary to those of Durst and co-workers who, using high-resolution electron microscopy, observed undulations in the smectic layer structure of a side-chain LC homopolymer.[21] Also, in our earlier study, we found that PS-HBPB diblocks with much lower LC content form onionlike morphologies consistent with Dupin Cyclides observed in S_C* focal conic superstructures.[3] Although some regions in PS-HBPB85 exhibit similar onionlike features, completely flat domains with long-range order are more commonly observed. The lack of curvature may be attributed to annealing-surface alignment effects throughout the 1 mm thick, solvent-cast film.

Thin Film Morphology. PS-HBPB85's thin film morphology was studied using AFM. Thin films were spun cast from toluene solutions onto precleaned silicon wafers and then annealed for 3 days under vacuum at 170 °C. Figure 5 shows an AFM image of the surface of an 18.4 nm thick film of PS-HBPB85. At the air interface, islands form with a thickness that corresponds to the block copolymer morphology. The cross-section depth profiles and histograms of depth distributions suggest that the film thickness varies in discrete steps of 5.8 nm for incommensurate film thickness. This dimension is lower than the bulk lamellar periodicity of 7.2 nm. The smaller periodicity in thin films can be explained by a larger smectic tilt angle arising from different anchoring conditions at the diblock−silicon interface. A more detailed study of thin film behavior of PS-HBPB85 and other high LC content diblocks is currently underway.

Thermal Behavior. The temperature dependence of PS-HBPB85's bulk morphology was also investigated. Temperature-dependent SAXS profiles are shown in Figure 6. The room-temperature Bragg peak appearing at a scattering vector $\mathbf{q} = 0.85$ nm^{-1} represents a *d* spacing of 72 Å, which corresponds to the lamellar microstructure observed in TEM; the second-order harmonic of this peak is also visible at $\mathbf{q} = 1.70$ nm^{-1}. Between 160 and 170 °C, the decrease in intensity of these two peaks marks the disappearance of the smectic bilayer lamellae and is just above an LC transition observed at 155 °C using differential scanning calorimetry. This transition is completely reversible—upon lowering the temperature both X-ray harmonics reap-

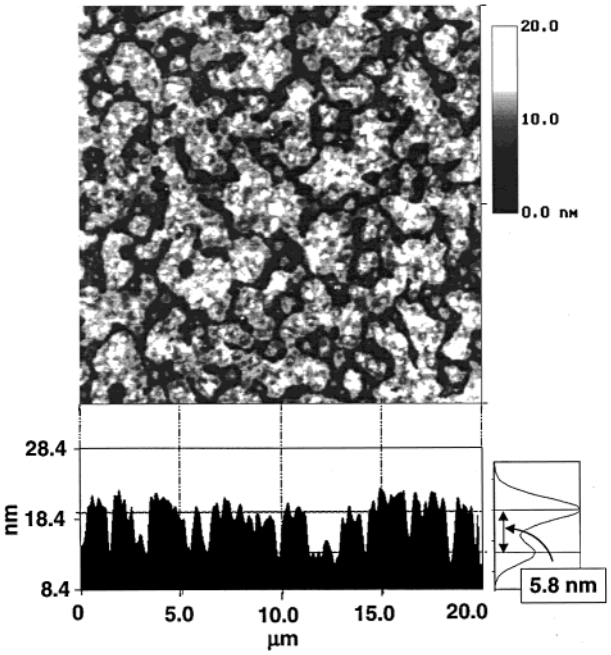

Figure 5. AFM micrograph ($20 \times 20\ \mu m^2$ viewing area) of an 18.4 nm thick film of PS-HBPB85. A typical cross-sectional profile is shown directly below the image; to the right of this profile is a histogram indicating the overall distribution of film thickness.

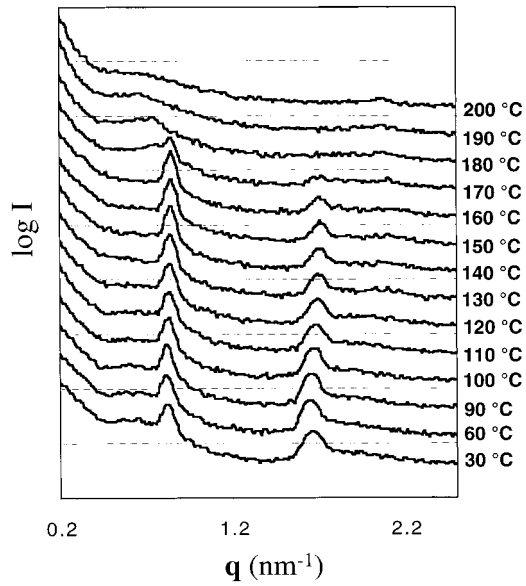

Figure 6. Temperature-dependent SAXS profiles of PS-HBPB85. Data are plotted as a function of the scattering vector $\mathbf{q} = (4\pi \sin \theta)/\lambda$, where θ is one-half of the scattering angle and λ is the X-ray wavelength.

pear with their original intensity. At temperatures immediately above the clearing point, a less intense, broader peak appears at $\mathbf{q} \sim 0.7\ nm^{-1}$ and is evidence of an order−order transition to an entirely different microstructure. Finally, at and above 200 °C, the intensity of the $\mathbf{q} \sim 0.7\ nm^{-1}$ peak disappears, as the diblock moves into a completely disordered phase.

Figure 7 shows TEM micrographs of the high-temperature phase obtained after rapidly quenching the sample from 180 °C. This temperature is above the LC clearing point and below the block copolymer ODT temperature. The quenched morphology consists of highly disordered PS spherical and ellipsoidal micro-

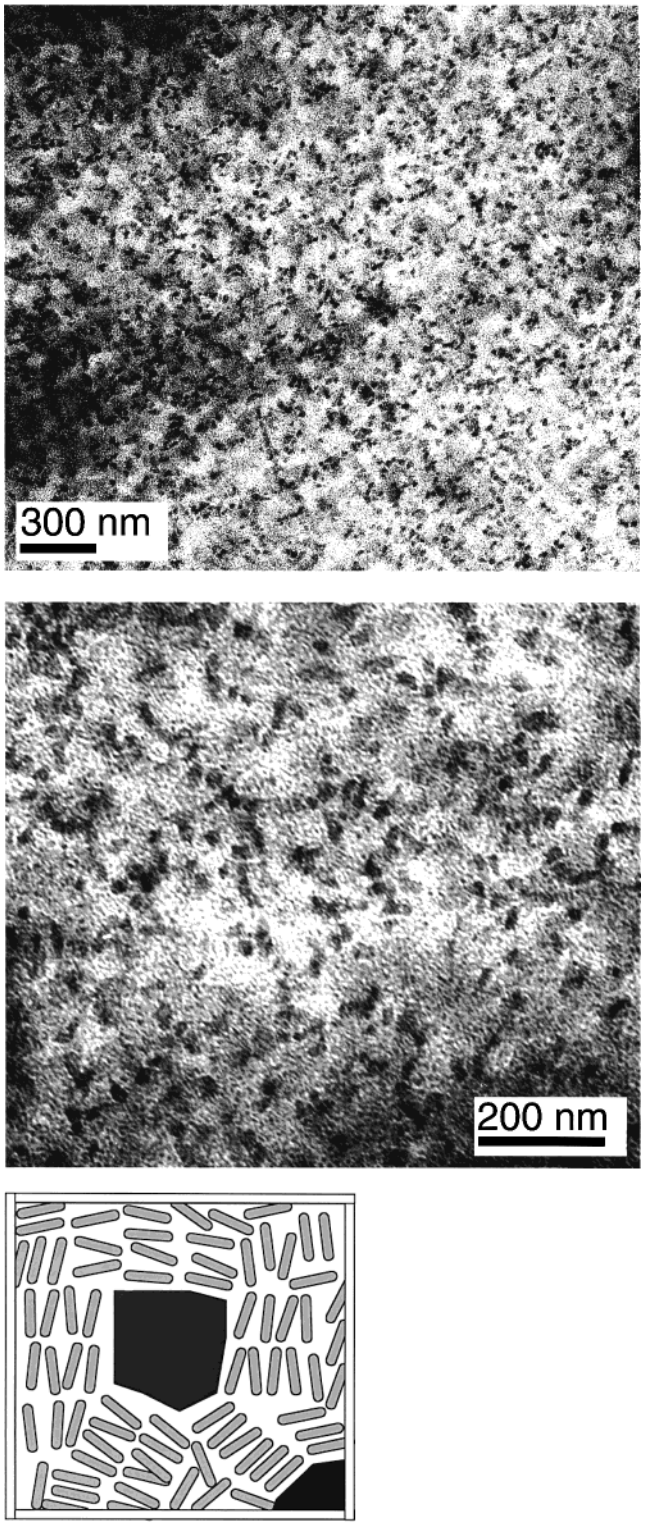

Figure 7. TEM micrographs of PS-HBPB85 after quenching from 180 °C. The inset is a cartoon illustrating how LC order influences the shape of the polystyrene domains.

domains that have cross-sectional diameters ranging from 20 Å, when viewed down a major axis, to 100 Å, when viewed from the minor axis. This dimension is consistent with the expected sphere diameter of 75 Å resulting from the volume of a single disk-shape domain in Figure 4. In some areas of Figure 7, the ellipsoids have begun to assemble into S_{C2} layers, driven by mesogenic ordering. The larger, dark patches measuring 200−300 Å are not single PS microdomains but consist

of clusters of PS domains viewed down their minor ellipsoid axes.

It is unclear whether, at 180 °C, PS-HBPB85's morphology consists of ordered or disordered spheres. It is possible that a high-temperature ordered phase may have existed, and upon cooling, as the side groups rapidly assembled into smectic layers, this order was lost. Indeed, the presence of a smectic substructure drastically influences the shape and structure of the diblock's morphology. For example, in Figure 7b, many of the PS domains have angular boundaries. As the figure inset suggests, these shapes arise from the order forced upon it by newly formed smectic planes.

PS-HBPB85's quenched morphology is reminiscent of a study on copolymer microstructure ordering dynamics carried out by Sakamoto et al.[22,23] Their TEM and SAXS analysis of SIS triblocks identified a lattice-disordering temperature (LDT). Below the LDT, the PS spherical microdomains order on a body-center-cubic (bcc) lattice, and above the LDT, the spheres exhibit short-range, liquidlike order. In PS-HBPB85, it is reasonable that above the LC clearing point, and below the order−disorder transition temperature, the morphology consists of PS spheres. A spherical phase would explain the presence of the lower-angle X-ray peak observed above 170 °C in Figure 6. This signal corresponds to a periodicity of 90 Å, and above 180 °C, the peak broadening suggests the diblock has entered a fully disordered state.

Recently, we reported the development of a free energy model to determine how LC−amorphous diblock copolymer morphology depends on composition and temperature.[24] Above T_{iso}, phases are asymmetric about $\phi_{LC} = 0.5$, and the model predicts a preference toward microstructures in which the amorphous block is in the center of the block copolymer micelles. This bias is due to architectural asymmetry—the LC block has a shorter contour length per unit volume and hence requires more energy to stretch than the amorphous block. Consequently, because of the inherent architectural asymmetry, the model predicts amorphous spheres just above T_{iso} for $\phi_{LC} > 0.76$.

Below T_{iso}, the model predicts two different morphological phase diagrams depending on how side groups are anchored to the intermaterial dividing surface (IMDS). For homeotropic anchoring, LC order encourages the backbone to extend parallel to the IMDS, and phases are preferred that have micelles with amorphous cores. Conversely, for planar anchoring, LC order facilitates stretching of the LC backbone orthogonal to the IMDS, thereby stabilizing phases in which the LC block is in the center of the copolymer micelles. The free energy model only considers constant-mean-curvature structures, i.e., lamellae, cylinders, and spheres, and it does not consider a disklike morphology. Interestingly, for planar anchoring, the free energy model predicts an LC induced order−order transition upon cooling from spheres to cylinders, and PS-HBPB85 exhibits a similar cooling transition from spheres to disklike structures. However, the free energy model predictions are for ideal systems and should not be compared directly to PS-HBPB85's proposed morphology. There are two major differences between the model and this experiment. First, the free energy model is based on nematics and does not account for the tendency of mesogens to form long-range, unidirectional smectic layers. Second, PS-HBPB85's proposed structure involves nonuniform anchoring conditions: the side groups are anchored planar to disk edges and are homoetropic to the top and bottom surfaces of the disks. Others studies of amorphous−LC diblocks have identified microstructures with nonuniform anchoring conditions at both low[8,25−28] and high LC compositions.[2,29−31] In each case, including PS-HBPB85, high-energy LC disclinations are avoided by forming unidirectional LC domains at the expense of greater interfacial surface free energy.

Link et al. have examined thin, free-standing films using depolarized reflected light microscopy and are able distinguish between anticlinic and synclinic junctions in S_{C2} homopolymer/monomer binary mixtures.[32] Following this venue, we are currently investigating the registry between smectic layers across the 1 nm thick PS disks, and we hope to characterize the electrooptic response of these materials. We are also studying the morphology of PS-HBPB85 in binary (homopolymer/LC block copolymer) blends.

Concluding Remarks

In summary, we have reported the first observation of a S_{C2} structure that is partitioned by disk-shaped microdomains of an amorphous−LC diblock copolymer. TEM, SAXS, and AFM analysis support the proposed structure and its unusual long-range order. At 85 wt % liquid crystal, the PS domains deform into disklike domains that arrange hexagonally between smectic bilayers. The bilayer periodicity was measured to be 72 Å using X-ray scattering, and from TEM the hexagonal lattice periodicity is estimated to be ∼150 Å. The formation of continuous smectic domains is the main driving force toward this morphology and takes precedence over the minimization of interfacial free energy. This result is consistent with our free energy model of SCLCBC's[24] and our earlier observations of PS-HBPB samples with lower LC volume fractions.[1]

Using temperature-dependent X-ray scattering and quenched TEM experiments, we have also shown that upon heating through 170 °C PS-HBPB85 exhibits an LC-induced order−order transition from the disklike S_{C2} morphology to the expected, spherical phase. This represents our second observation of a thermoreversible LC-induced order−order transition in these materials. In our earlier work, we reported a sample with 58 wt % LC content, PS-HBPB58, that undergos a similar transition from a predominately lamellar, perforated morphology, to a completely lamellar phase. These studies have revealed that the LC domain has stronger influences on morphology at high LC compositions where there is a driving force to form continuous LC domains.

On another note, we have also shown that short PS blocks can be used to directly observe smectic layer formation through TEM. This, or a similar approach, may be useful in characterizing other complicated LC defects and superstructures.

Acknowledgment. The authors acknowledge the National Science Foundation Polymer Program for funding under Grant DMR-9526394. We are also grateful for helpful discussions with Rick Register and Ned L. Thomas. Special acknowledgments are given to Andres A. Tamez of MIT for his experimental contributions to this work.

References and Notes

(1) Anthamatten, M.; Hammond, P. T. *Macromolecules* **1999**, *32*, 8066−8076.

(2) Anthamatten, M.; Zheng, W. Y.; Hammond, P. T. *Macromolecules* **1999**, *32*, 4838−4848.
(3) Zheng, W. Y.; Hammond, P. T. *Macromolecules* **1998**, *31*, 711−721.
(4) Adams, J.; Gronski, W. *Makromol. Chem., Rapid Commun.* **1989**, *10*, 553−557.
(5) Zaschke, B.; Frank, W.; Fischer, H.; Schmutzler, K.; Arnold, M. *Polym. Bull.* **1991**, *27*, 1−8.
(6) Yamada, M.; Iguchi, T.; Hirao, A.; Nakahama, S.; Watanabe, J. *Polym. J.* **1998**, *30*, 23−30.
(7) Osuji, C. O.; Chen, J. T.; Mao, G.; Ober, C. K.; Thomas, E. L. *Polymer* **2000**, *41*, 8897−8907.
(8) Omenat, A.; Hikmet, R. A. M.; Lub, J.; van der Sluis, P. *Macromolecules* **1996**, *29*, 6730−6736.
(9) Chiellini, E.; Galli, G.; Angeloni, A. S.; Laus, M.; Bignozzi, M. C.; Yagci, Y.; Serhatli, E. I. *Macromol. Symp.* **1994**, *77*, 349−358.
(10) Zheng, W. Y.; Hammond, P. T. *Macromol. Rapid Commun.* **1996**, *17*, 813−824.
(11) Leibler, L. *Macromolecules* **1980**, *13*, 1602−1617.
(12) Gallot, B.; Lenclud, A. L. *Polymer* **1997**, *38*, 3493−3499.
(13) Gallot, B.; Monnet, F.; He, S. *Liq. Cryst.* **1995**, *19*, 501−509.
(14) Gallot, B.; Lenclud, A. L.; He, L. *J. Appl. Polym. Sci.* **1997**, *65*, 2407−2417.
(15) Chiellini, E.; Dossi, E.; Galli, G.; Solaro, R. *Macromol. Chem. Phys.* **1995**, *196*, 3859−3875.
(16) Bignozzi, M. C.; Angeloni, S. A.; Laus, M.; Incicco, L.; Francescangeli, O.; Wolff, D.; Galli, G.; Chiellini, E. *Polym. J.* **1999**, *31*, 913−919.
(17) Percec, V.; Heck, J.; Ungar, G. *Macromolecules* **1991**, *24*, 4957−4962.
(18) Zheng, W. Y.; Albalak, R. J.; Hammond, P. T. *Macromolecules* **1998**, *31*, 2686−2689.
(19) Wu, J. S.; Fasolka, M. J.; Hammond, P. T. *Macromolecules* **2000**, *33*, 1108−1110.
(20) Sentenac, D.; Demirel, A. L.; Lub, J.; de Jeu, W. H. *Macromolecules* **1999**, *32*, 3235−3240.
(21) Durst, H.; Voigt-Martin, I. G. *Makromol. Chem., Rapid Commun.* **1986**, *7*, 785−790.
(22) Sakamoto, N.; Hashimoto, T.; Han, C.; Kim, D.; Vaidya, N. *Macromolecules* **1997**, *30*, 1621.
(23) Sakamoto, N.; Hashimoto, T. *Macromolecules* **1998**, *31*, 8493−8502.
(24) Anthamatten, M.; Hammond, P. T. *J. Polym. Sci., Part B: Polym. Phys.*, in press.
(25) Fischer, H.; Poser, S.; Arnold, M.; Frank, W. *Macromolecules* **1994**, *27*, 7133−7138.
(26) Fischer, H.; Poser, S.; Arnold, M. *Liq. Cryst.* **1995**, *18*, 503−509.
(27) Ruokolainen, J.; Saariaho, M.; Ikkala, O.; ten Brinke, G.; Thomas, E. L.; Torkkeli, M.; Serimaa, R. *Macromolecules* **1999**, *32*, 1152−1158.
(28) Ruokolainen, J.; ten Brinke, G.; Ikkala, O. *Adv. Mater.* **1999**, *11*, 777−780.
(29) Fischer, H.; Poser, S.; Arnold, M. *Macromolecules* **1995**, *28*, 6957−6962.
(30) Mao, G.; Wang, J.; Ober, C.; Brehmer, M.; O'Rourke, M.; Thomas, E. *Chem. Mater.* **1998**, *10*, 1538−1545.
(31) Osuji, C.; Chen, J.; Mao, G.; Ober, C.; Thomas, E. *Polymer* **2000**, *41*, 8897−8907.
(32) Link, D. R.; Clark, N. A.; Ostrovskii, B. I.; Soto Bustamante, E. A. *Phys. Rev. E* **2000**, *61*, R37−R40.

MA011168N